# Simultaneous, Submicron Infrared and Raman Microspectroscopies for Effective Failure and Contamination Analyses

Michael Lo[1], Mustafa Kansiz[1], Eoghan Dillon,[1] Jay Anderson,[1] Curtis Marcott[2]
[1] Photothermal Spectroscopy Corp., 325 Chapala St., Santa Barbara, CA 93101, USA
[2] Light Light Solutions LLC, P.O. Box 81486, Athens, GA 30608, USA
Phone : (+1) 805-845-6568, Email : mike@photothermal.com

***We demonstrate the analysis of ~1 µm contamination with high signal-to-noise in a simultaneous infrared and Raman microscope at the same time, at the same location and at submicron spatial resolution. This combined technique provides high sensitivity to small sample volumes without melting or damaging the samples by using separate infrared excitation and visible laser detection mechanisms. The measurement process does not involve physically contacting the sample, hence simplifying sample preparation and avoiding cross-contamination between sample changes. To showcase this new capability, we provide examples from the contamination in the gap between a solder joint and a non-wetting pad, adhesive residues on a glass panel and foreign matter near a copper post. Such challenges could not be readily resolved with conventional FTIR and Raman techniques. The simultaneous O-PTIR and Raman brings complementary and confirmatory results to analysis previously thought to be difficult to impossible.***

***Keywords—infrared, O-PTIR, FTIR, Raman, simultaneous, contamination, failure analysis, non-wetting, foreign matter, chemistry, submicron, diffraction-limited, Rayleigh criterion, Mie scattering, open circuit, residue***

## I. INTRODUCTION

For the past half a century, Fourier Transform infrared (FTIR) spectrometry has provided the industry with an unrivalled chemical analysis capability [1]. Since the IR spectrum can provide a chemical "fingerprint" of a material, and because modern FTIR microspectrometers are relatively easy to use, the technique has been well-positioned for identifying unknowns. While these are good qualities, conventional FTIR spectrometry relies on direct detection of the diffraction-limited infrared light from the source that was not absorbed by the sample. This effectively limits the resolving power to 5-20 µm [2], depending on the wavelength of interest. For microelectronics failure and contamination problems, region of interests (ROI) and foreign materials (FM) are typically less than 5 µm in physical dimensions, rendering FTIR spectrometry ineffective in spatially resolving their chemistry. For this reason, FTIR is mostly reserved for probing organic material greater than 30 µm in size. The use of an attenuated total reflectance (ATR) accessory could improve the practical wavenumber dependent spatial resolution to about 1-5 µm [1,3] with a germanium internal reflection element (IRE), but intimate contact between the probe and the sample is required; hence leading to potentially irreversible sample damage and possible cross-contamination between specimens. Certainly, the IRE could be damaged as well. FTIR spectra collected in transmission mode are considered the true absorption spectra and sample thickness would need to be less than 10-20 µm; but most, if not all, microelectronics samples cannot be thinned feasibly into the said dimension. FTIR in reflection mode could be a non-contact option for analysing these thick samples but spectral distortion due to refraction index related changes and scattering processes will be the dominant factor in rendering spectra nearly useless [1]. In particular, the sharp edges of microelectronic components can cause significant scattering and dispersion artefacts that further distort the resulting reflection spectra. Similar effects could be seen in changing the form factor from a film to increasingly small spheres of the same material [4].

FTIR spectroscopy is more sensitive to polar bond vibrations, whereas Raman spectroscopy is more sensitive to non-polar vibrations – hence the complementarity of the two techniques. Raman makes use of a single excitation laser, typically at 532 or 785 nm, which gives a theoretical spatial resolution of 1 µm or less as per Rayleigh criterion [1,3]. The non-contact, standoff data collection is highly desirable for microelectronics failure analysis (FA), without requiring of thin sectioning. Raman scattering cross-sections are much smaller than IR absorption cross-section by about 8 orders of magnitude [5], therefore, higher laser power excitation is needed to generate signals and thus increases the probability of damaging samples [6]. Finally, many samples display auto-fluorescence that can often overwhelm the weak Raman intensities, which in turn reduces the utility of the spectra [7].

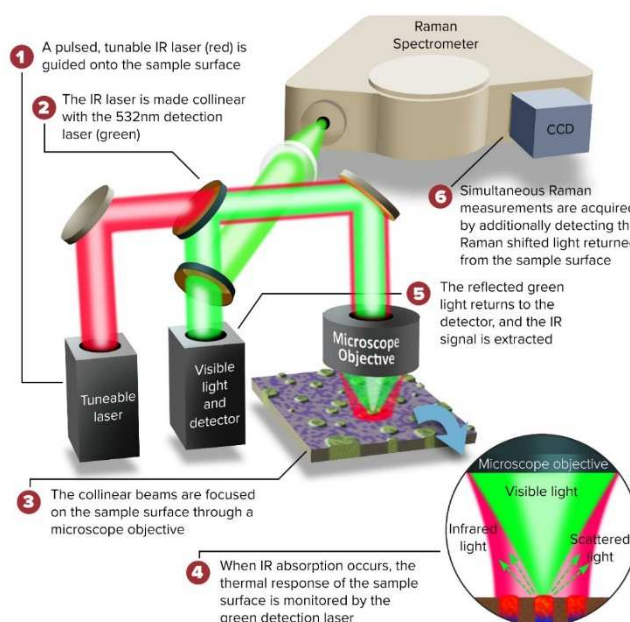


Fig. 1. Schematic of the simultaneous O-PTIR and Raman (IR+Raman) instrument.

The strength of **O**ptical **P**hoto**T**hermal **I**nfra**R**ed Spectroscopy (O-PTIR) stems from directly detecting the localized photothermal effect due to absorption of infrared light [8]. In contrast, conventional FTIR spectrometry

calculates the absorption spectra by ratioing the sample and the background signals. Small absorption cross-sections and short sample path lengths would lead to miniscule changes in the intensity of the incoming beam, leading to noisy spectra. A schematic of the O-PTIR technique is shown in Fig. 1, where a quantum cascade laser (QCL) emits IR laser pulses that excite the sample and a second co-linearized visible probe laser (532 nm) detects the resulting photothermal effects due to absorption of IR. With this pump-probe arrangement, O-PTIR is extremely sensitive to small masses even below 400 femtograms (equivalent to a single 900 nm polystyrene sphere) [9]. No FTIR spectra could be generated for such isolated particles in transmission mode nor with an ATR accessory. More recently, optical photothermal systems could further extend sensitivity to a single 300 nm virus particle [10]. With O-PTIR, the illumination and detection are conducted in a non-contact manner with a shorter wavelength visible laser, which gives Raman-like diffraction-limited spatial resolution that is also wavenumber independent across the entire mid-infrared tuning range [11]. Instead of detecting the sample at 1000 $cm^{-1}$ (10 μm) with a theoretical spatial resolution of 12 μm (0.5 NA objective) in the mid-infrared, the O-PTIR technique detects the IR absorption with its 532 nm probe laser, which would equate to a theoretical spatial resolution of *ca.* 416 nm by Rayleigh's criterion. Most importantly, despite collecting IR absorption data in non-contact reflection mode, band distortions from Mie scattering artefacts and spectral interference are absent in O-PTIR spectra. Therefore, O-PTIR spectra are directly searchable in current commercial and customized infrared databases for identification of the unknowns. Despite using a visible laser for detection, sample auto-fluorescence does not influence the quality of O-PTIR spectra. Finally, O-PTIR spectra with good signal-to-noise could be collected even at IR laser power levels less than 100 μW, thereby reducing the probability of sample damage. These characteristics bring about convenient sample analysis in infrared wavelengths without the limitation of FTIR. In essence, simultaneous O-PTIR and Raman spectroscopies achieve the holy grail of conducting complementary and confirmatory analyses at the same time, same point and at the same spatial resolution in one click while significantly reducing manpower required for extensive sample preparation and from operating separate FTIR and Raman instruments.

## II. Discussion

The O-PTIR technique revolutionizes the approach of failure and contamination analyses on microelectronics for organic matter by providing wavenumber-independent submicron spatial resolution in a non-contact reflection mode. In the subsequent case studies, the inherently rough and rigid samples would have been difficult for conventional FTIR in transmission or ATR modes. For the ATR mode, the rough surface prevents good contact with the smooth probe surface, leading to band distortion and artefacts that are hard to correct and interpret. Transmission mode is not available due to the thick opaque sample substrate. Raman microscopy could provide a feasible alternative with its high spatial resolution and the non-contact data acquisition modes. The Raman technique would satisfy some of the samples which do not exhibit significant fluorescence. When neither FTIR nor Raman yields useful results, those samples would be referred to elemental analysis, which lacks information with regards to the arrangement of chemical bonds. The complementary and simultaneous O-PTIR and Raman dataset taken at the same spot and the same time provide analysis that would have been impossible in the past. All samples have been received and analyzed as-is, in the mIRage+R Simultaneous Infrared and Raman microscope (Photothermal Spectroscopy Corp., Santa Barabara, CA).

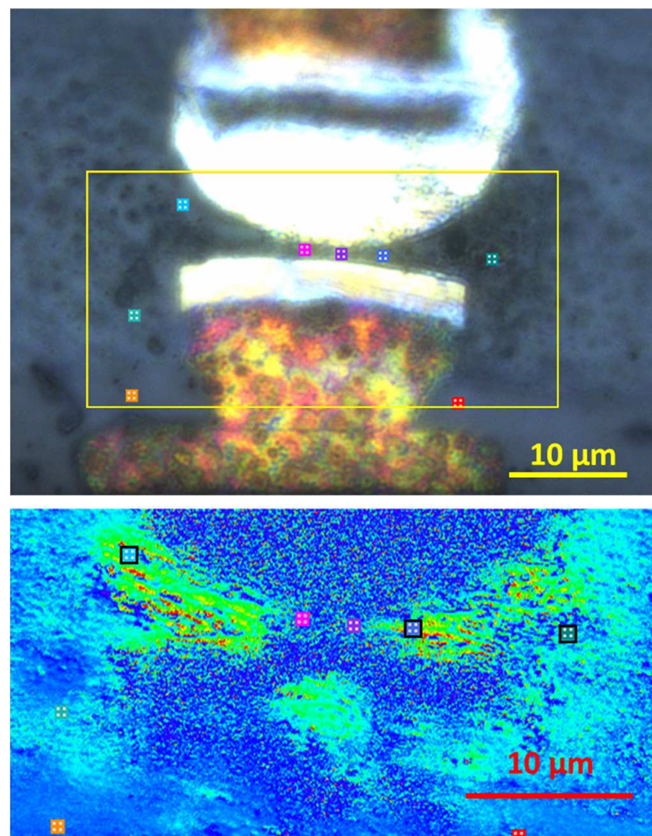


Fig. 2 (Top) Optical image of a open circuit due to a non-wetting solder joint; (Bottom) the corresponding image of O-PTIR infrared intensity ratio of 1672 $cm^{-1}$ to 1452 $cm^{-1}$ that shows the distribution of carboxylates at and around the gap; markers indicate the approximate locations where the experimental data are recorded in Fig. 3 and Fig. 4.

### A. *Opened circuit due to an organic contamination present on a non-wetting metal pad surface*

Simultaneous O-PTIR and Raman spectroscopies provide high resolution chemical analysis where the region of interest (ROI) is shorter (1-2 μm) than the infrared wavelengths of 5-10 μm. Fig. 2 represents a scenario where there are hard metallic contacts with an exceedingly small gap with trapped organic material between them. In the ratioed O-PTIR image of the ROI, strong infrared absorption signal at 1672 $cm^{-1}$ is notable in the 10 μm x 5 μm bright green regions on both sides of the gap. The optical image shows significant presence of dark spots in between the beaded solder and the aluminum pad below. There, the two blue O-PTIR spectra in Fig. 3 are consistent with carboxylates, which could include surfactants and ionized abietic acid typically found in flux. Since O-PTIR absorption intensity is directly proportional to localized photothermal effects, the non-zero baseline of O-PTIR spectra reflects a broad absorption characteristic of the sample that is consistent with the carbonized and/or metallized materials. The magenta and purple (C-1) spectra reveal the chemistry of the 1 μm gap. The narrow 1708 $cm^{-1}$ shoulder on the high wavenumber side of the broad 1672 $cm^{-1}$ band is consistent with saturated free carboxylic

acid [12]. The broad absorption band around 1100 $cm^{-1}$ is also consistent with glycol-based rheology modifier material present in solder flux formulation [13]. Spectrum C-1 is similar to the blue ones, suggestive of carboxylates and carbon-rich residues; the latter is confirmed with the broad 1598 and 1360 $cm^{-1}$ Raman shifts for polycrystalline carbon in Spectrum C-1R of Fig. 4 [14]. As expected, outside of this contamination zone, the O-PTIR and Raman spectra in teal (C-2) are consistent with silica-based underfill (Si-O, broad 1110 $cm^{-1}$) and the ones in red/orange are consistent with the polyimide solder mask. Simultaneous O-PTIR and Raman spectroscopies clearly demonstrate the value of having complementary dual IR and Raman spectra for confirming the chemical nature of the unknown, even in localized submicron spaces typical of microelectronics failure analysis.

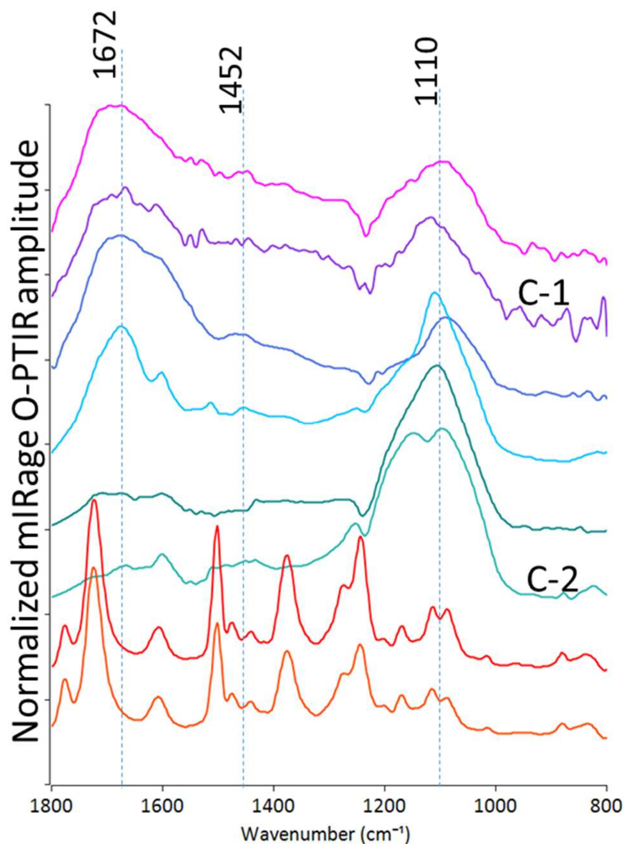


Fig. 3. O-PTIR spectra within the ROI as shown in Fig. 2.

*B. Adhesive residue on glass panel*

The surface sensitive nature of the O-PTIR technique enables analysis of microscopic contamination on glass substrates. With conventional infrared microspectroscopy, infrared spectra would have been dominated by glass – signals from relatively small residues are often overwhelmed. As a potential alternative, ATR-FTIR could limited the sample volume by taking advantage of the evanescent wave penetration of 0.66 µm for Ge or 2.0 µm (at 1000 $cm^{-1}$) for diamond IREs [1]. Still, their physical contact requirement with the glass sample could damage the glass substrate, making ATR-FTIR a potentially destructive technique. The high NA of the objective used in O-PTIR significantly tightens the effective zone to within 1-3 µm in the vertical z-direction, thus tightly confining the measurement zone toward the surface. This mechanism increases sensitivity from the adhesive residue and minimizes contributions from the underlying glass substrate. The top optical image in Fig. 5 shows spots of adhesive residues scattered across a 50 µm x 50 µm space on glass panel, which was a larger format sample with dimensions of 20 cm x 20 cm. Due to the large spot size of conventional FTIR microscopy, infrared signals from the adhesive would have been averaged out by the underlying substrate.

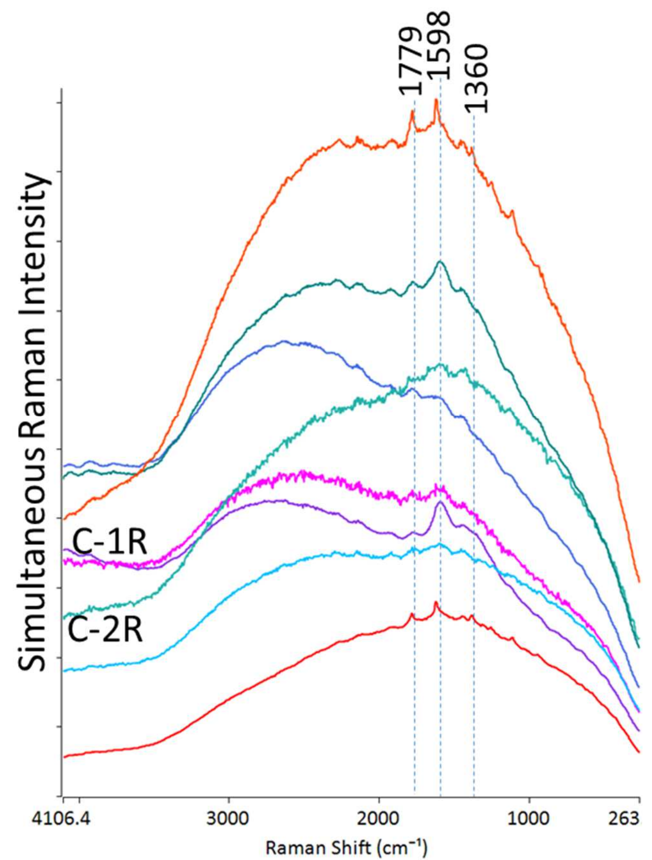


Fig. 4. Corresponding simultaneous Raman spectra taken at the same time and at the same spot as O-PTIR spectra in Fig. 3.

Using the point-and-shoot function in the data acquisition software, O-PTIR spectra reveal heterogenous nature of the residue in spite of the signal contribution from glass (Fig. 6). The intensities of absorption bands around 1736 $cm^{-1}$ and 1162 $cm^{-1}$ are varying independent of the 1640 $cm^{-1}$ and 1550 $cm^{-1}$. This observation suggests there are at least two major components within the adhesive residue: a mixture of acrylate [15] and a polyamide [16]. The yellow marker region represents the most isolated and intense acrylate region (strong 1736 $cm^{-1}$ but little 1640 $cm^{-1}$) while the orchid-colored marker for the polyamide region (little 1736 $cm^{-1}$ but strong 1640 $cm^{-1}$).

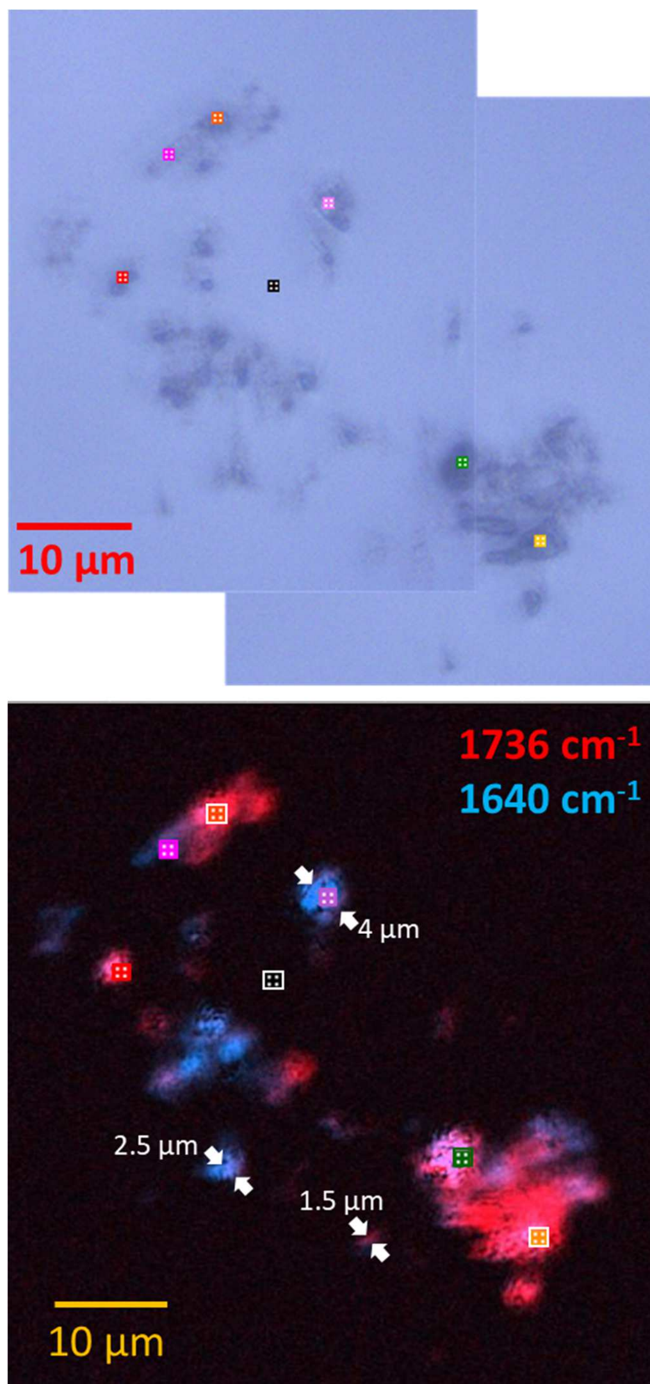


Fig. 5. Optical image (Top) and overlaid O-PTIR image taken at 1736 and 1640 $cm^{-1}$ (Bottom) illustrating the distribution of adhesive residue left behind on a glass substrate.

O-PTIR single frequency chemical imaging of the same area reveals and confirms the spectroscopic analysis above. The overlaid O-PTIR image in Fig. 5 shows some of the smaller residues are on the order of 1-5 µm and their relative distribution could be readily discerned. Each IR image (1736 $cm^{-1}$ and 1640 $cm^{-1}$) takes approximately eight minutes per wavenumber at 50 nm pixel in x and 100 nm pixel in y. In the red regions overlapped with the red and orange markers, acrylate (C=O stretch at 1736 $cm^{-1}$; C-O-C stretch at 1162 $cm^{-1}$) is the dominant species; in the blue regions overlapped with purple and magenta markers, polyamide (amide-I at 1640 $cm^{-1}$ and amide-II at 1558 $cm^{-1}$) is the major component; purple regions overlapped with the green marker are where both the acrylate and polyamide are present. The relative absorption band intensity changes between these two groups of frequencies are proportional to the relative concentration differences between the two components. In this case, the components may have phase separated or poorly mixed, leading to the deposition of adhesive residues. The high sensitivity of the O-PTIR technique directly enable the identification of possible failure modes of the adhesive, thereby improving the process and appeal of the final product.

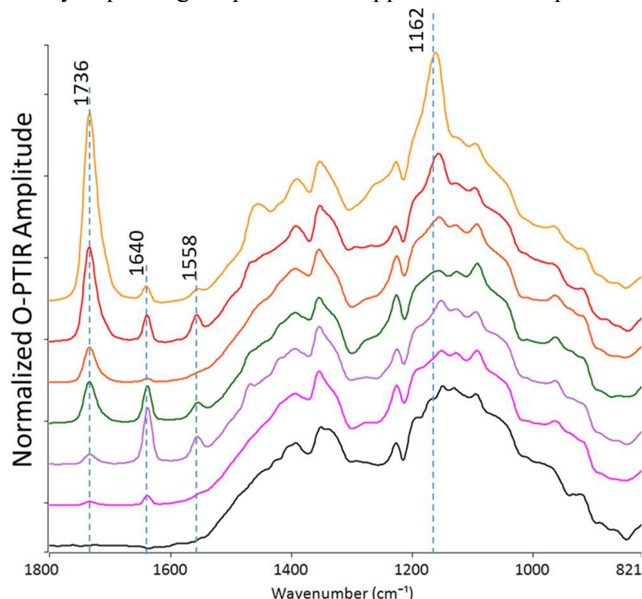


Fig. 6. O-PTIR spectra taken at marker locations demonstrating the presence of multiple species in the adhesive residue on a glass panel as showing Fig. 5.

Finally, the O-PTIR technique provide highly sensitive, spatially resolved infrared-based chemical analysis that can be arduous for conventional infrared techniques. In transmission mode of FTIR, the high optical density of silicon dioxide around the Si-O antisymmetric stretch band around 1087 $cm^{-1}$ would require film thickness of less than 1 µm to avoid being optically dark and to avoid distorting its band shapes [17,18]. The O-PTIR spectra of silicon dioxide is not saturated despite obtaining spectral data from thick glass samples. The fine structure within the Si-O can still be studied. The state of the glass, e.g., chemistry, mechanical strain in the silicon dioxide band, can be studied as part of a failure analysis process or for research development. The versatility of the O-PTIR instrument will find applications that are previously not achievable with conventional FTIR spectroscopy.

### *C. Contamination in the underfill near a copper post*

In this final demonstration, the O-PTIR technique enables chemical analysis of chemo-mechanical polished specimen that used to be arduous due to their rough surface. These sample surfaces are unsuitable for the reflection mode of FTIR due to significant scattering of IR light. Although the dimension of the contamination appears sufficiently large for conventional FTIR analysis, the hard sample surface presented in Fig. 7 prevents good contact between the surface and a micro-ATR probe. Without making a good contact with the sample surface, those ATR-FTIR spectra are expected to be sufficiently distorted [19]. Raman could not

provide useful information due to the presence of strong fluorescence baseline and the sample could be easily damaged by high excitation power level. Energy-dispersive X-ray spectroscopy (EDS or EDAX) represents a typical next-in-line analysis and could effectively suggest its elemental composition. Still, the technique would be short of providing information about bond arrangements, unlike infrared spectroscopy.

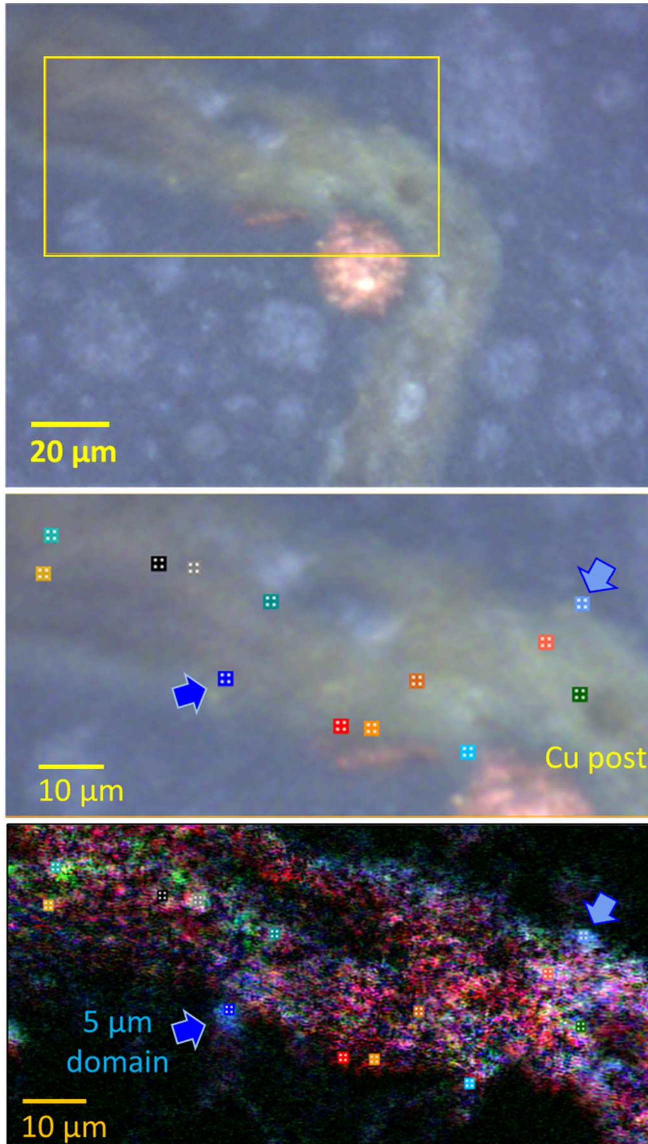


Fig. 7. (Top) Optical image showing the yellowed contamination spot near the copper post, which has been chemo-mechanically polished; (Middle) area imaged by O-PTIR in the bottom panel; (Bottom) the corresponding overlaid O-PTIR image illustrating the heterogeneity of the contamination taken at 1724 (red) 1598 (blue) and 1460 (green) $cm^{-1}$

Using the gentle pump-probe nature as presented in O-PTIR, infrared-based chemical identification can be obtained without damaging sample while providing IR spectra that are searchable against commercial IR databases and images in submicron spatial resolution. Spatially resolved spectroscopic information could be extracted from the heterogenous mixture as shown in Fig. 8. Near the blue spots, the spectra contain both the fillers (1110 $cm^{-1}$) and foreign material (1598 $cm^{-1}$) being consistent with a carboxylate [12]. Within the contamination boundary, it is widely enveloped by a strong and broad absorption centering around 1724 $cm^{-1}$, which is consistent with free carboxylic acids in addition to a smaller proportion of the carboxylates at 1598 $cm^{-1}$. The center peak of the free carboxylic acid has been blue-shifted by about 16 $cm^{-1}$ from an aliphatic free carboxylic acid. Such shift could be due to halogenation of the carboxylic acids [12]. Unpublished EDS data of the contamination supports this hypothesis: significant presence of chlorine atoms has been detected within the boundary of the contamination. Hotspots of 1460 $cm^{-1}$ absorption are consistent with long chain aliphatic material and scattered unevenly within the yellow tinged contamination. The variable nature of the relative band heights at these wavenumbers suggests these are independent components.

The submicron spatial resolution of the O-PTIR technique enables spatially resolved chemical analysis of a complex contamination mixture (at least three species) by combining O-PTIR imaging and spectroscopic analyses. The technique significantly reduces sampling area, thus increasing sensitivity towards the localized spectroscopic differences instead of averaging out the difference over a larger sampling volume as expected from conventional FTIR microspectroscopy. Finally, the undistorted, normal-appearing spectra enable direct interpretation of spectroscopic information without fitting spectra into complex mathematical algorithms. The presence of uneven surface with hard underfill and copper posts do not hinder a thorough infrared-based O-PTIR analysis.

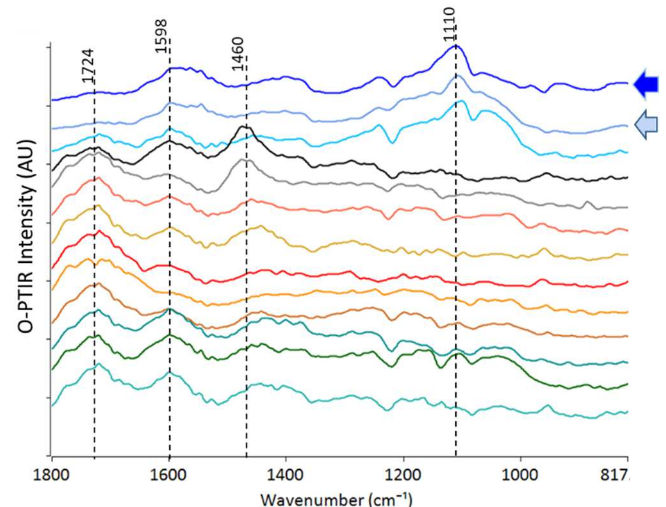


Fig. 8. Corresponding O-PTIR spectra taken within the area confirming the heterogeneity of the chemical species within the contaminated area as shown in Fig. 7.

## III. Conclusion

In this report, we have demonstrated high spatial resolution simultaneous O-PTIR and Raman spectroscopy enabling chemical analysis of challenging failure and contamination analyses on microelectronic specimens. The narrowest analyzable dimension of the feature could be as small as 1 µm in between a solder bump and a non-wetting metal solder pad. With dual (O-PTIR and Raman) channels of data, we can confidently identify the contamination as a mixture of carboxylates, carboxylic acids and disordered carbon. The O-PTIR technique can also identify scattered micron-sized adhesive residues as a heterogeneously

distributed acrylate and polyamide on a glass panel, which would have dominated the conventional FTIR spectrum instead of the adhesive components. Finally, a contamination sample next to copper posts could be analyzed by the gentle pump-probe based O-PTIR to learn of its multicomponent nature, which was not possible by Raman due to its light-sensitive characteristic nor with ATR-FTR due to its rough sampling surface. For a very long time, these impossible sample types have been challenging due to inherently hard and rough surface morphologies, foreign matter of less than 5 μm, the presence of glass, spectral distortion and strong auto-fluorescence upon excitation. Analytical strategy in microelectronics failure and contamination analyses are destined to change with the simultaneous, submicron O-PTIR and Raman microspectroscopy.

## REFERENCES


[1] P. R. Griffiths, J. A. de Haseth. "Fourier Transform Infrared Spectrometry." 2nd Ed. 2007.

[2] J.A. Bailey, R.B. Dyer, D.K. Graff, J.R. Schoonover. "High Spatial Resolution for IR Imaging Using an IR Diode Laser. *Appl. Spectr.* 2000, *54*, 159.

[3] K.L.A. Chan, S.G. Kazarian. "New Opportunities in Micro- and Macro-Attenuated Reflection Infrared Spectroscopic Imaging: Spatial Resolution and Sampling Versatility." *Appl. Spectr.* 2003, *57*, 381.

[4] P. Bassan, H.J. Byrne, F. Bonnier, P. Dumas, P. Gardner. 'Resonant Mie Scattering in Infrared Spectroscopy of Biological Materials – Understanding the "Dispersion Artefact."' *Analyst*, 2009, *134*, 1586.

[5] Y. Bai, Yin, J., Cheng, J-x. "Bond Selective Imaging by Optically Sensing the Mid-Infrared Photothermal Effect." Sci. Adv. 2021, 7, pp. eabg1559.

[6] M.J. Pelletier, C.C. Pelletier. Raman Spectroscopy. 2nd Ed. 2005.

[7] J. Zhao, H. Lui, D.I. McLean, H. Zeng. "Automated Autofluorescence Background Subtraction Algorithm for Biomedical Raman Spectroscopy." *Appl. Spectr.* 2003, *61*, 1225.

[8] D. Zhang, C. Li, C. Zhang, M.N. Slipchenko, G. Eakins, J.-x. Cheng. "Depth-resolved Mid-Infrared Photothermal Imaging of Living Cells and Organisms with Submicrometer Spatial Resolution." *Sci. Adv.* 2016, *2,* e1600521.

[9] M. Lo, C. Marcott, M. Kansiz, Dillon, E., C. Prater. "Sub-micron, Non-contact, Super-resolution Infrared Microspectroscopy for Microelectronics Contamination and Failure Analyses." 2020 IEEE International Symposium on the Physical and Failure Analysis of Integrated Circuits (IPFA), July 2020, 68.

[10] Zhang, et. al. "Vibrational Spectroscopic Detection of a Single Virus by Mid-Infrared Photothermal Microscopy." *Anal. Chem*. 2021, *93*, pp4100-4107.

[11] Kansiz, et. al. "Optical Photothermal Infrared Microspectroscopy with Simultaneous Raman – A New Non-Contact Failure Analysis Technique for Identification of <10 μm Organic Contamination in the Hard Drive and other Electronics Industry," *Microscopy Today*, May 2020, 26.

[12] Roeges, N.P.G. "Guide to the Complete Interpretation of Infrared Spectra of Organic Structures." 1997.

[13] K. Ryder, A. Ballantyne, R. Harris, C. Zaleski. "Solder Flux. US Patent App. US20170157717A1.

[14] Tuinstra, F., Koenig, J. L. "Raman Spectrum of Graphite." *J. Chem. Phys*. 1970, *53*, 1126.

[15] J. Zhang, X. Zheng, Q. Ma. "Performance Study on Acrylic Pressure-Sensitive Modified with Metakaolin. *IOP Conf. series: Materials Science and Engineering*," 2020, *711*, 012053.

[16] K. Liu, Y. Li, L. Tao, R. Xiao. "Preparation and characterization of polyamide fiber based on a phosphorous-containing flame retardant." *RSC Adv*., 2018, *8*, 9261.

[17] J.E. Dial, R.E. gong, J.N. Fordemwalt. "Thickness Measurements of Silicon Dioxide Films on silicon by Infrared Absorption Techniques." *J. Electrochem. Soc.* 1968, *115*, 326.

[18] W. Bensch, W. Bergholz. "An FT-IR Study of Silicon Dioxides for VLSI Microelectronics." *Semicond. Sci. Technol*. 1990, *5*, 421.

[19] A.A. Stolov, D.A. Simoff. "Application of Micro-Attenuated Total Reflectance Infrared Spectroscopy to Quantitative Analysis of Optical Fiber Coatings: Effects of Optical Contact." *Appl. Spectr*. 2006, *60*, 29.